MATHEWS Open Access Journals

ISSN 2474-6843

Research Article | Mathews Journal of Dentistry

Morphological Characterization of Human Dental Enamel Irradiated with Er:YAG Laser using the Statistical Functions

Ştefan Ţălu[1], Rosalía Contreras-Bulnes[2], Laura Emma Rodríguez-Vilchis[2], Gonzalo Montoya-Ayala[3].

[1]Technical University of Cluj-Napoca, Faculty of Mechanical Engineering, Department of AET, Discipline of Descriptive Geometry and Engineering Graphics, 103-105 B-dul Muncii St., Cluj- Napoca 400641, Cluj, Romania.

[2]Universidad Autónoma del Estado de México, Facultad de Odontología, Centro de Investigación y Estudios Avanzados en Odontología, México, C.P. 50130, México.

[3]Universidad Nacional Autónoma de México, Facultad de Odontología, Laboratorio de Biología Periodontal y Tejidos Mineralizados, México

Corresponding Author: Dr. Rosalía Contreras–Bulnes Universidad Autónoma del Estado de México, Facultad de Odontología, Centro de Investigación y Estudios Avanzados en Odontología, México, C.P. 50130, México. **Tel:** (52)7222124351, **Fax:** (52)7222126464, **e-mail:** rcontrerasb@uaemex.mx

Received Date: 20 Jan 2016
Accepted Date: 11 Mar 2016
Published Date: 16 Mar 2016

Citation: Ştefan Ţălu, Contreras-Bulnes R, Rodríguez-Vilchis LM and Montoya-Ayala G. (2016). Morphological Characterization of Human Dental Enamel Irradiated with Er:YAG Laser using the Statistical Functions. M J Dent 1(1): 005.

ABSTRACT

Purpose

The aim of this study was to estimate the effect of irradiation with the Er:YAG laser on the surface nanomorphology of human dental enamel using the statistical functions. The surface nanomorphology was recorded by atomic force microscopy (AFM), and the data were estimated by statistical functions.

Materials and methods

Two samples of human dental enamel were divided into two groups: a) group I was irradiated with the Er:YAG and no water irrigation with next 25.5 J/cm^2 energy density; b) group II was the control (no laser irradiation or control). The nanomorphology changes were observed by AFM in contact mode, in air, on square areas of topography on the 1 µm × 1 µm. Based on AFM data and applying the computational algorithms, the statistical functions were plotted.

Results

The local scale properties of human dental enamel at nanometric level were estimated with the statistical functions. The graphical results showed the local and global non-uniformity of the surface patterns. The one way analysis of variance (ANOVA) was performed ($P < 0.05$) to distinguish significant differences among the groups.

Conclusions

The computational algorithm indicated that the surface nanomorphology differ significantly of these two groups. AFM and the statistical functions applied for surface roughness provide important information about the surface nanomorphology to characterize of non-uniform micro-distributions from the 3-D surface of the human dental enamel.

KEYWORDS

Atomic Force Microscopy; Human Dental Enamel; Er:YAG Laser Image Analysis, Statistical Functions; Surface Nanomorphology; Surface Roughness.

INTRODUCTION

Biominerals are a subset of the mineral kingdom, those created by living creatures. Among them, enamel is the hardest mineralized biological tissue, about 96 wt% (weight percentage) mineral in the form of crystallites of hydroxyapatite, 3 wt% water and and 1 wt% organic [1]. The enamel surface presents a variable appearance, exhibiting features such as aprismatic enamel, perikymata, prism-end markings, cracks, pits and elevations [2]. Furthermore, it has been reported that local factors in the enamel surface

produce changes, such as those associated to oral habits, including toothbrushing, use of toothpastes, consumption of various beverages, as well as dental procedures between them, fluoride application, bleaching, etching agents and laser irradiation [3-13].

The Er:YAG laser is well absorbed by all biological tissues that contain water molecules, its use was approved in 1997 by the U.S. Food and Drug Administration (FDA) [14,15]. In dentistry, it is a versatile laser prescribed for the treatment of soft tissues and ablation of hard ones [14]. In addition, an early report suggested that enamel adjacent to the ablated area by Er:YAG laser irradiation exhibited an increase in acid resistance [16]. Several in vitro studies on smooth dental enamel surfaces concur that Er:YAG laser irradiation promotes caries prevention and produce morphological changes as revealed by SEM. However, the 3-D (three-dimensional) surface topographic features at nanometres level studied by Atomic force microscopy (AFM) have been scarcely evaluated [11-13, 17-21].

Application of the fractal and multifractal geometry has been used successfully in last years for numerical characterization of 3-D topography of human dental enamel surfaces [21-24].

It is known that, the fractal and multifractal analyses have also been used to quantitatively characterize the 3-D rough surfaces in the field of dental materials [25-29].

The main purpose of this study was to investigate the effect of irradiation with the Er:YAG laser on the surface nanomorphology of human dental enamel and the resulting changes in crystal structures. The sample 3-D surfaces were examined by atomic force microscopy (AFM) and the data were estimated by statistical functions.

MATERIALS AND METHODS

Tooth Selection and Sample Preparation

The protocol of this study was reviewed and approved by the Research and Ethics Committee at the Autonomous University of the State of Mexico (UAEM).

Caries-free bicuspid teeth extracted for orthodontic reasons from patients aged 15–17 years old, who reported no use of fluoride products other than fluoride toothpaste, were obtained with the patients informed consent. Teeth with caries, restorations, cracks, and defects in the structure or color of the enamel on the buccal surfaces or fluorosis were excluded.

Immediately after extraction, teeth were collected in 0.2 (wt/vol) thymol solution at 277 K for one month until the experiment was performed. Enamel fluorescence was evaluated with a laser fluorescence caries detection system DIAGNOdent® pen (DIAGNOdent, KaVo, Biberach, Germany), 2 teeth with sound enamel (values of 0-13, according to the manufacturer's specifications) were included in the study [30,31].

Each tooth was fixed with a thermoplastic epoxy resin (Allied High Tech Products, Rancho Dominguez, CA, USA) to a glass slide. Then, the crown was removed using a diamond disc (BesQual, New York, USA) mounted on a low-speed motor (Micromotor M2 Master, M25800011, Drillco Devices Ltd., Miami, FL, USA) under constant distilled water irrigation.

Afterwards, a diamond wheel saw (South Bay Technology, Inc., San Clemente, CA, USA) mounted on a cutter (South Bay Technology, Inc., USA) was used to obtain the samples under constant irrigation. One block (3 × 3 mm) from buccal surface was obtained from each tooth (one for group). Subsequently, all samples were rinsed (with deionized water) and dried at room temperature previous to AFM evaluation. The sample sizes was 1 × 1 mm.

Er:YAGLaser Irradiation

For the irradiation of the specimens, an Er:YAG laser system (Lumenis OPUS DUO™ Er:YAG + CO_2, Yokneam, Israel) was employed, with a wavelength fixed at 2.94 µm, at an energy output from 100 to 200 mJ, frequency of 10 Hz, pulse duration of 250-400 msec, and an exit tip diameter from 1.0 to 1.3 mm.

As shown in Table 1, two slides of human dental enamel were divided into two groups: (n = 15, regions of interest (ROI) on each group. These ROI were selected through a random process from the AFM images obtained at next step.

Groups (n = 15 regions of interest on each group)	Energyoutput	Diameter of the tip	Energy density	Water irrigation conditions
I (laser irradiation)	200 mJ	1.0 mm	25.5 J/cm^2	No irrigation
II (no laser irradiation or control)	-	-	-	-

Table 1: Details of the experimental and control groups tested in the study.

The energy levels were calibrated by the calipers of the equipment. A power meter (LaserMate-P, Coherent Co., Santa Clara, CA) was employed to measure periodically the energy delivered. The surface was scanned once by hand (18 sec) with the sapphire tip of the laser perpendicular to it, at a working distance of 1 mm and with distilled water irrigation (5.0 mL/m).

Atomic Force Microscopy

AFM images were obtained of 2 samples (1 control and 1 irradiated) by Jeol JSPM 4210 Atomic Force Microscope. For this purpose, tapping mode, in air, with ultrasharp silicon cantilever (NSC 15, type A) was employed with the following specifications: length (125 µm), width (35 µm), thickness (4 µm), resonance frequency (325 kHz) and constant applied force (40 N/m).

The images were acquired with 256 x 256 pixels resolution and a scanning rate of 1 Hz from scanning square areas of 1 x 1 µm^2. For AFM image processing and analysis of the structures, Custom algorithms developed in Matlab were used. The experiments were done in the same room, at room

temperature (298 ± 1K) and (44 ± 1%) relative humidity.

Statistical Analysis

All data were analyzed using the SPSS 18.0 statistical package (SPSS Inc., Chicago, IL, USA). The measurements were analyzed using the Kolmogorov–Smirnov test to assess the distribution of the data. Afterwards, the one way analysis of variance (ANOVA) was employed for comparison among groups; if significant differences were found, Bonferroni or Tamhane's T2 post-hoc tests were used, depending upon Levene's test of homogeneity of variance. In all statistical analysis, the level of significance was stated at $P < 0.05$.

Statistical Functions

For the complete description of the 3-D surface properties it is necessary to study higher order functions. Usually, second-order statistical quantities observing mutual relationship of two points on the surface are employed. The statistical functions are namely the autocorrelation function (ACF), the height-height correlation function (HHCF), and the power spectral density function (PSDF) [32].

In our study we also used the radial ACF $G_r(\tau)$ i.e. angularly averaged two-dimensional ACF, which of course contains the same information as the one-dimensional ACF for isotropic surfaces [32]. On the other hand, we used the radial PSDF $W_r(K)$, i.e. angularly integrated two-dimensional PSDF, which of course contains the same information as the one-dimensional PSDF for isotropic rough surfaces [32].

In our study, the computational analysis of the AFM files was performed on each region of interest (ROI), based on the original algorithm and the determined graphs were in correlation with ISO 25178-2: 2012 [32,33].

RESULTS

The representative 3-D AFM images, for scanning square areas of the samples from the two groups (Table 1), are shown in Figure 1, a, b: a) group I and b) group II. They are shown in 3-D mode, with the vertical height scale bar (in nanometers [nm]) displayed on the right side of the AFM image. Scanning square areas of 1 µm x 1 µm.

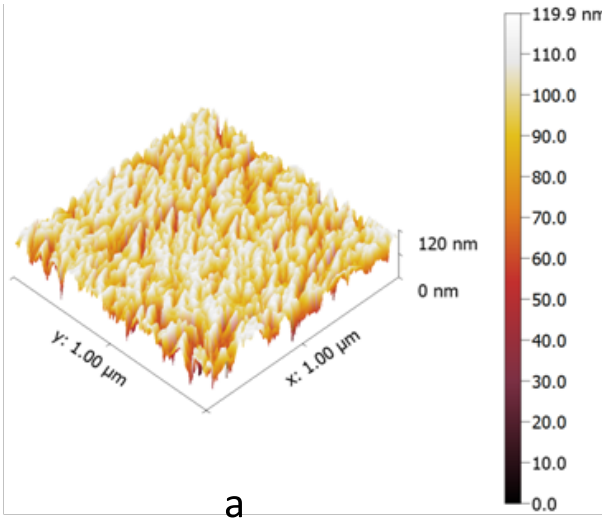

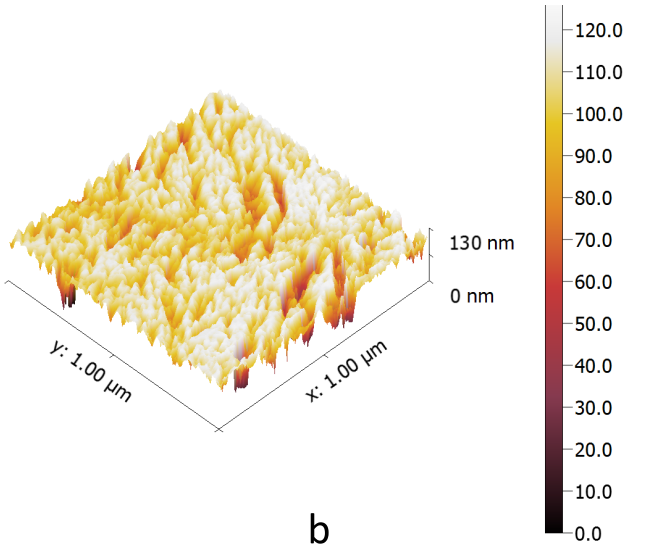

Figure 1: A set of representative AFM images (top and 3-D view), for scanning square areas of the samples from each group (Table 1), are shown in Figure 1, a, b: a) group I and b) group II. They are shown in 3-D mode, with the vertical height scale bar (in nanometers [nm]) displayed on the right side of the AFM image. Scanning square areas of 1 µm x 1 µm.

Group I has the most regular surface (Figure 1). This is qualitatively seen in Figure 1, a: image for group I has a lot of flat areas in comparison with group II.

In Figure 2 are shown the ACF, HHCF, and PSDF functions for samples of Figure 1, in horizontal direction, for: a) group I; b) group II. Scanning square areas of 1 µm x 1 µm.

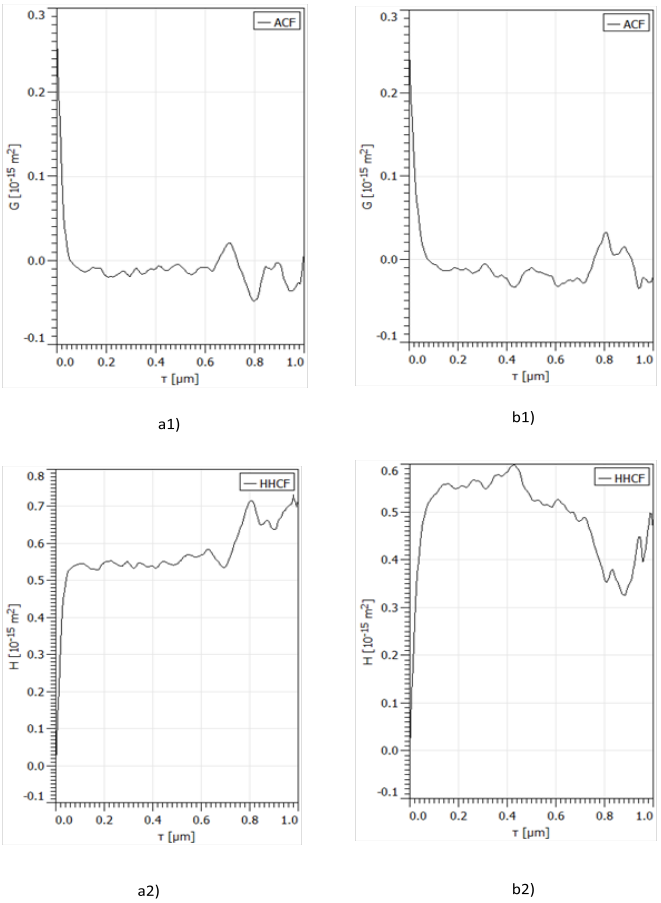

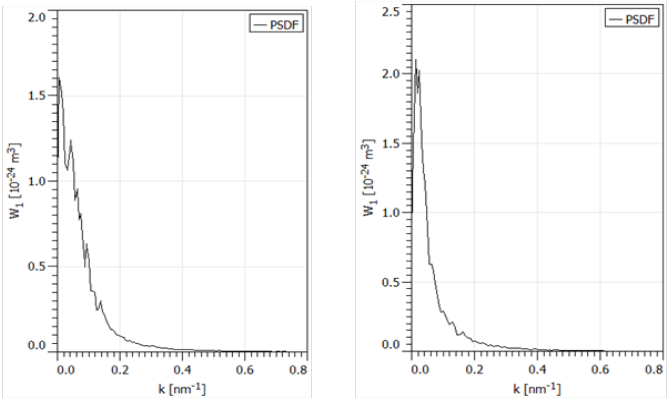

Figure 2: The ACF, HHCF and PSDF functions for samples of Figure 1, in horizontal direction, for: a) group I; b) group II. Scanning square areas of 1 µm x 1 µm.

In Figure 3 are shown the ACF, HHCF and PSDF functions for samples of Figure 1, in vertical direction, for: a) group I; b) group II. Scanning square areas of 1 µm x 1 µm.

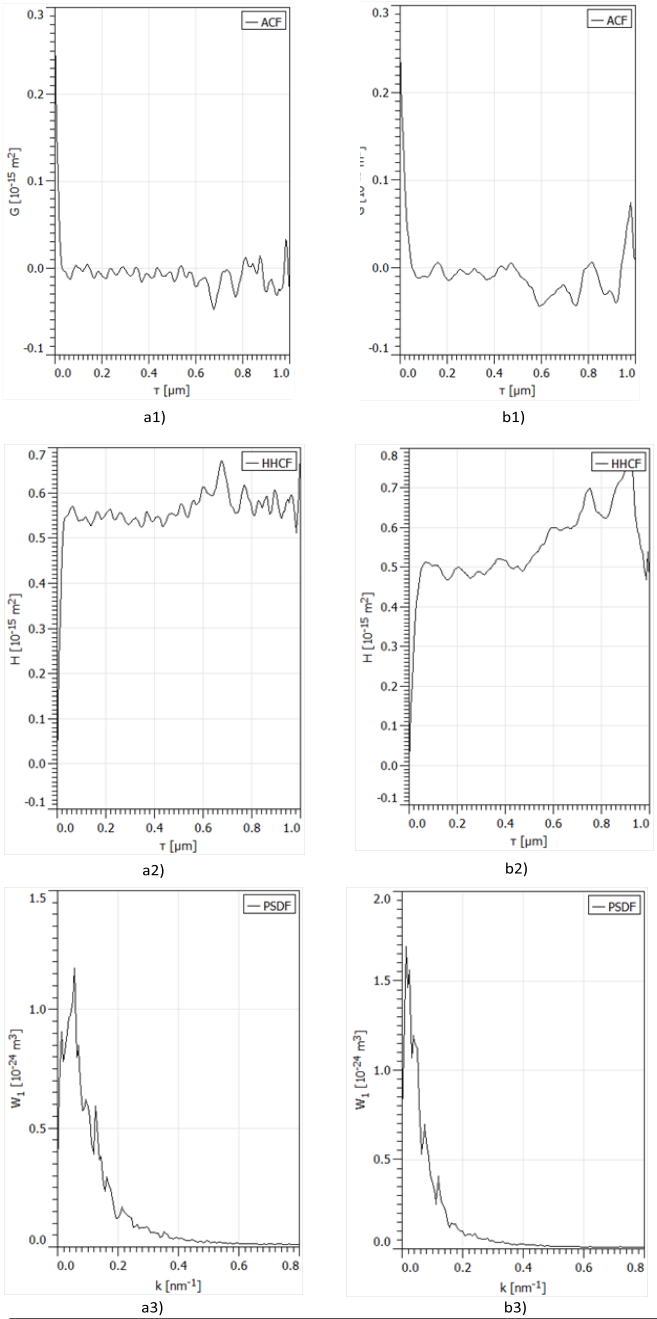

Figure 3: The ACF, HHCF and PSDF functions for samples of Figure 1, in vertical direction, for: a) group I; b) group II. Scanning square areas of 1 µm x 1 µm.

In Figure 4 are shown the radial ACF and radial PSDF functions for samples of Figure. 1, for: a) group I; b) group II. Scanning square areas of 1 µm x 1 µm.

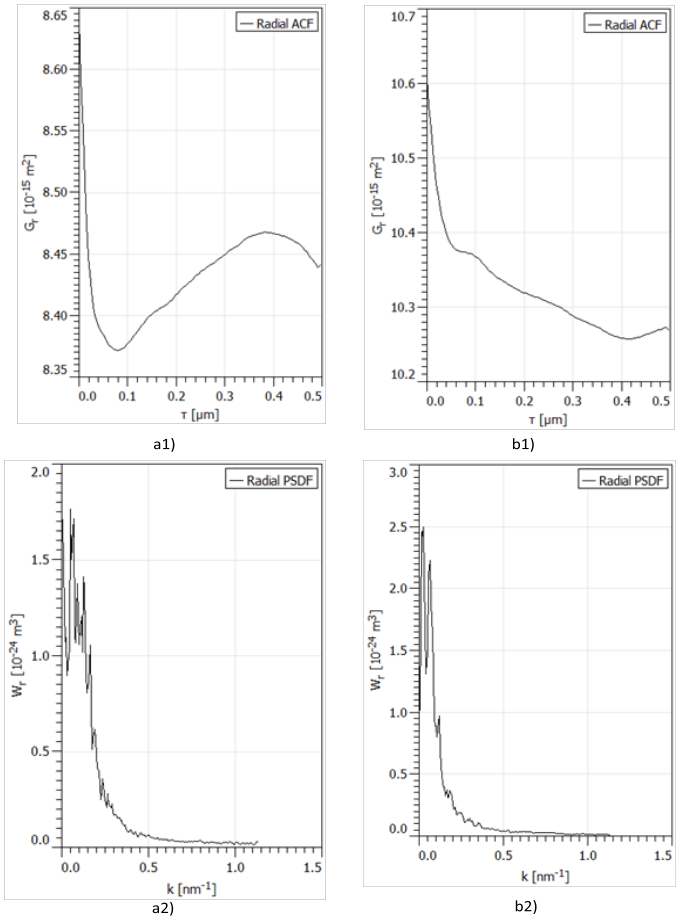

Figure 4: The radial ACF and radial PSDF functions for samples of Figure 1, for: a) group I; b) group II. Scanning square areas of 1 µm x 1 µm.

As shown in Table 2, the computational algorithm indicated that surface nanomorphology differ significantly of these two groups.

The basic properties of the height values distribution of the surface samples	Group I	Group II
(Sa) [nm]	15.8	12.3
(Sq) [nm]	19.2	16.3
Skewness (Ssk) [-]	-1.20	-1.65
Kurtosis (Sku) [-]	0.94	4.30
Average inclination θ [°]	24	49
Average inclination ϕ [°]	-0.51	-10.57
Relative projected area of hills, [%]	58	60

Table 2: The basic properties of the height values distribution (including its variance, skewness and kurtosis) of the surface samples, for scanning square areas of 1 µm x 1 µm. Statistically significant difference for all values: $P < 0.05$.

DISCUSSION

AFM, the statistical surface roughness parameters, and multifractal analysis are useful tools for providing information about the 3-D surface nanomorphology of human dental enamel irradiated with an Er:YAG laser and optimal surface characteristics in order to characterize its structural 3-D microrelief [21].

There are no previous reports regarding to surface morphology evaluation of human dental enamel irradiated with Er:YAG laser, using the statistical functions.

After the analysis of AFM images from the two groups, it can be seen that each preparation protocol is associated with a specific topography. This type of topography is characterized by a significant heterogenity of sample surfaces (random distributions with elevations and local irregularities between nano-asperities) in a 3-D surface map, as a result from their preparation protocol process and it can be characterized by the statistical functions employed.

The surface of group I was more regular, comparative with the other group, it could be explained by melting and subsequent homogeneous recrystallization resulting from the heat generated by laser irradiation, with a degree of asymmetry *A* for group I closer to 0.7. Moreover, the surface nanomorphology of Er:YAG laser irradiation (under group I conditions) was the most regular when multifractal analysis was carried out [21].

On the other hand, group II (no irradiated enamel) have a large area of closed enamel prism in the surface, attributable to the natural organization of this tissue, with the minimum value of *A*. Also, two grooves were present in the no irradiated surface, observed as irregularities.

Investigation results indicated that the relationships between the surface micromorphology and the preparation protocol, and their determining are important, as the surface micromorphology has a significant effect on the surface features and clinical behaviour in the oral environment.

It should be taken into consideration that random distributions and localized irregularities also characterized the irradiated surface. Along these areal damages, some local damages could be detected. Final surface morphology of human dental enamel depends on the protocol type, and on a choice of optimal variant requires a deeper insight on the 3-D surface patterns quality.

CONCLUSION

Investigations carried out confirm that the surface roughness can be described by statistical functions and provide valuable information in characterization and comparison of 3-D microrelief peculiarities of human dental enamel.

These types of analyses provide a basis for additional research and analysis with 3-D methods in medical image analysis and computer graphics.

ACKNOWLEDGMENTS

The authors thank Dr. David Villanueva Jurado and Dr. Israel Ramírez López, Maxillofacial Surgeons from the Clínica Odontológica Morelos, Instituto de Salud al Servicio del Estado de México y Municipios (ISSEMYM), for their assistance with obtaining the samples. This project was financed by Universidad Autónoma del Estado de México (UAEM) and Universidad Nacional Autónoma de México (UNAM).

DECLARATION OF INTEREST

Neither author has a financial or proprietary interest in any material or method mentioned. All authors read and approved the final manuscript.

REFERENCES

1. Skinner HCW. (2005). Biominerals. Mineral Mag. 69(5), 621-641.

2. Berkovitz BKB, Moxham BJ, Linden RWA and Sloan AJ. (2011). Master Dentistry Volume Three Oral Biology. China: Elsevier. 144.

3. Lussi A, Lussi J, Carvalho TS and Cvikl B. (2014). Toothbrushing after an erosive attack: will waiting avoid tooth wear? Eur J Oral Sci. 122(5), 353-359.

4. Ozalp S and Tulunoglu O. (2014). SEM-EDX analysis of brushing abrasion of chitosan and propolis based toothpastes on sound and artificial carious primary enamel surfaces. Int J Paediatr Dent. 24(5), 349-357.

5. Hara AT, Barlow AP, Eckert GJ and Zero DT. (2014). Novel in-situ longitudinal model for the study of dentifrices on dental erosion-abrasion. Eur J Oral Sci. 122(2), 161-167.

6. Jensdottir T, Arnadottir IB, Thorsdottir I, Bardow A, et al. (2004). Relationship between dental erosion, soft drink consumption, and gastroesophageal reflux among Icelanders. Clin Oral Investig. 8(2), 91-96.

7. Zamudio-Ortega CM, Contreras-Bulnes R, Scougall-Vilchis RJ, Morales-Luckie RA, et al. (2014). Morphological and chemical changes of deciduous enamel produced by Er:YAG laser, fluoride, and combined treatment. Photomed Laser Surg. 32(5), 252-259.

8. Klarić E, Marcius M, Ristić M, Sever I, et al. (2013). Surface changes of enamel and dentin after two different bleaching procedures. Acta Clin Croat. 52(4), 419-429.

9. Ogiwara M, Miake Y and Yanagisawa T. (2008). Changes in dental enamel crystals by bleaching. J. Hard Tissue Biol. 17(1), 11-16.

10. Zanet CG, Arana-Chavez VE and Fava M. (2006). Scanning electron microscopy evaluation of the effect of etching agents on human enamel surface. J ClinPediatr Dent. 30(3), 247-250.

11. Díaz-Monroy JM, Contreras-Bulnes R, Olea-Mejía OF, García-Fabila MM, et al. (2014). Chemical changes associated with increased acid resistance of Er:YAG laser irradiated enamel. Scientific World Journal. 501357.

12. Díaz-Monroy JM, Contreras-Bulnes R, Olea-Mejía OF, Rodríguez-Vilchis LE, et al. (2014). Morphological changes produced by acid dissolution in Er:YAG laser irradiated dental enamel. Microsc Res Tech. 77(6), 410-414.

13. Rodríguez-Vilchis LE, Contreras-Bulnes R, Olea-Mejía OF, Sánchez-Flores I, et al. (2011). Morphological and structural changes on human dental enamel after Er:YAG laser irradiation: AFM, SEM, and EDS evaluation. Photomed. Laser Surg. 29(7), 493-500.

14. Aoki A, Sasaki KM, Watanabe H, and Ishikawa I. (2004). Lasers in nonsurgical periodontal therapy. J. Periodontol 2000. 36, 59-97.

15. Sulewski JG. (2000). Historical survey of laser dentistry. Dent. Clin. North Am. 44(4), 717-752.

16. Kayano T, Ochiai S, Kiyono K, Yamamoto H, et al. (1989). Effects of Er:YAG laser irradiation on human extracted teeth. Kokubyo Gakkai Zasshi. 56(2), 381-392.

17. Castellan CS, Luiz AC, Bezinelli LM, Lopes RM, et al. (2007). In vitro evaluation of enamel demineralization after Er:YAG and Nd:YAG laser irradiation on primary teeth. Photomed. Laser Surg. 25(2), 85-90.

18. Cecchini RCM, Zezell DM, de Oliveira E, de Freitas PM, et al. (2005). Effect of Er:YAG laser on enamel acid resistance: morphological and atomic spectrometry analysis. Lasers Surg. Med. 37(5), 366-372.

19. Apel C, Meister J, Gotz H, Duschner H, et al. (2005). Structural changes in human dental enamel after subablative erbium laser irradiation and its potential use for caries prevention. Caries Res. 39(1), 65-70.

20. Rodríguez-Vilchis LE, Contreras-Bulnes R, Sánchez-Flores I and Samano EC. (2010). Acid resistance and structural changes of human dental enamel treated with Er:YAG laser. Photomed. Laser Surg. 28(2), 207-211.

21. Ţălu Ş, Contreras-Bulnes R, Morozov IA, Rodríguez-Vilchis LE, et al. (2015). Surface nanomorphology of human dental enamel irradiated with an Er:YAG laser. Laser Physics. 26(2).

22. Morozov IA, Svistkov AL, Gileva OS and Erofeeva ES. (2010). Experimental investigation of the influence of bleaching on enamel surface microstructure. Russ. J. Biomech. 14(1), 56-63.

23. Ţălu Ş. (2015). Micro and nanoscale characterization of three dimensional surfaces. Basics and applications. Napoca Star Publishing House, Cluj-Napoca, Romania.

24. Morozov IA, Belyaev AYu, Izyumov RI, Erofeeva ES, et al. (2013). Impact of whitening on the microstructure of human tooth enamel. Inorganic Materials: Applied Research. 4(1), 71-76.

25. Ţălu Ş, Stach S, Alb SF and Salerno M. (2015).Multifractal characterization of a dental restorative composite after air-polishing. Chaos, Solitons & Fractals. 71, 7-13.

26. Ţălu Ş, Stach S, Lainović T and Vilotić M (2015). Surface roughness and morphology of dental nanocomposites polished by four different procedures evaluated by a multifractal approach. Appl Surf Sci. 330, 20-29.

27. Ţălu Ş, Patra N and Salerno M. (2015). Micromorphological characterization of polymer-oxide nanocomposite thin films by atomic force microscopy and fractal geometry analysis. Progress in Organic Coatings. 89, 50-56.

28. Ţălu Ş, Stach S, Klaić B, Mišić T, et al. (2015). Morphology of Co-Cr-Mo dental alloy surfaces polished by three different mechanical procedures. Microsc. Res. Tech. 78(9), 831-839.

29. Berezina S, Il'icheva AA, Podzorova LI, Ţălu Ş. (2015). Surface micromorphology of dental composites [CE-TZP] - [AL_2O_3] with Ca^{+2} modifier. Microsc. Res. Tech. 78(9), 840-846.

30. Shinohara T, Takase Y, Amagai T, Haruyama C, et al. (2006). Criteria for a diagnosis of caries through the DIAGNOdent. Photomed Laser Surg. 24(1), 50-58.

31. Zandoná AF and Zero DT. (2006). Diagnostic tools for early caries detection. J Am Dent Assoc. 137(12), 1675-1684.

32. Gwyddion software user guide, version 2.28, (2012) © P. Klapetek, D. Necas, C. Anderson, Czech Metrology Institute, Brno, Czech Republic.

33. ISO 25178-2: 2012 Geometrical product specifications (GPS) - Surface texture: Areal - Part 2: Terms, definitions and surface texture parameters.